1wp

X-644-72-161
PREPRINT
NASA TM X- 65942

PARTICLE SHAPE AND MAGNETIZATION OF CHONDRITE METEORITES LUNAR SAMPLES AND IMPACTITES

PETER WASILEWSKI

JUNE 1972

GSFC — GODDARD SPACE FLIGHT CENTER —
GREENBELT, MARYLAND

Particle Shape and Magnetization of Chondrite Meteorites, Lunar Samples, and Impactites

Peter Wasilewski*

Planetology Branch
Goddard Space Flight Center
Greenbelt, Maryland 20771

*Research Associate Professor at George Washington University, Washington, D.C.

I

Abstract:

Extra terrestrial materials, certain materials which have their origin at the earth's surface due to meteoritic impact, or under highly reducing conditions, such as in the case of basaltic flows in contact with coal beds or serpentenites, all contain Fe and FeNi phases with high magnetization values and spherical shape. Normally, the demagnetizing field (H_D=NI_S:where N is the demagnetizing factor and Is the saturation magnetization) is corrected for. However, in disperse systems, such as most natural materials, we do not make this correction, and instead the particle shape effects are analyzed in terms of the saturation fields, $Hs=H_D=NI_S$, and the magnetization differences (ΔI_S). Discrete size modes of superparamagnetic (SP), multidomain (MD), and single domain (SD) particles result in reduced coercive force (Hc), increase in the value R_H (=ratio of remanent coercive force, H_R, to H_c), and decrease in the value R_I (ratio of remanent magnetization, I_R, to saturation magnetization, I_S). The main distinctions between the various natural materials can be made by this approach. Hysteresis loops for terrestrial basalts, Fe and Ni rods and spheres, chondrite meteorites, lunar samples, impactites, and chondritic fusion crust are presented.

Introduction:

Natural materials, with the exception of iron meteorites and terrestrial ores are dispersed ferromagnetics, i.e. grains of ferromagnetic material dispersed in a nonmagnetic silicate matrix or other nonmagnetic matrix. In extra terrestrial materials, impactites and certain terrestrial rocks, such as basaltic flows in contact with coal beds or trees and serpentenites, Fe and Fe alloy phases are found which have high magnetization values and add a significant magnetic grain shape aspect to the sample.

Collisions in outer space, impact at planetary surfaces, atmospheric heating, and *in situ* oxidation of landed meteorites will affect the ferromagnetic assemblage in these natural materials. Almost nothing is known about the magnetic property changes associated with such processes. The utilization of magnetic hysteresis analysis has great promise (a) in evaluating different meteorite classes, (b) in evaluating the black fusion crust on chondrite meteorites, (c) in evaluating the grain size and shape distribution in natural materials, (d) in evaluating the magnetic coercivity distribution, and (e) in evaluating the thermal, oxidative, and shock alterations in natural materials. This paper will demonstrate the effective utilization of magnetization measurements in evaluating magnetic property changes

associated with thermochemical and thermomechanical alterations of the magnetic phases in natural ferromagnetic materials.

Measurements and Mineral Phases:

The principle reasons for making magnetic measurements are : (a) evaluation of type, shape, and size of ferromagnetic phases, (b) evaluation of chemical and mechanical alterations of the mineral phases, (c) establishment of a thermomechanical classification of chondrites, lunar rocks, and impactites, based on magnetic properties, and (d) evaluation of remanent magnetism and the possible information embodied in any component. The initial step in such a program is the characterization of the sample. Since FeNi particles are present in extra terrestrial samples the role of these phases must be evaluated.

Magnetic hysteresis loops and magnetization curves were measured on a vibrating sample magnetometer located at the U.S. Steel Research Laboratory. Fields up to 16 K.Oe. were used. Samples of various natural and man made materials were studied: polycrystalline steel spheres (SAE 52100), nickel wire (99.99% purity), shocked FeNi alloys (8% Ni - 164 kb shock), crossed nickel wires, two sphere configurations, chondrite fusion crust, carbonaceous chondrites, chondrules from the Allende and Chainpur chondrites, 30 ordinary chondrites with varying degrees

of atmospheric degradation, shock, and shock heating. Published and unpublished data on the lunar rocks and fines are also considered.

In the chondrite meteorites, ferromagnetic mineral phases are present which cover a Curie point range of ~500° C. The significant mineral phases influencing magnetization curves are FeNi. Various natural processes, such as cooling, oxidation, high temperature alterations and shock induced deformation will alter the phase composition and structures and the effective particle size and shape. Previous work on chondritic meteorites by Stacey et al. (1961) has shown that "Fe_3O_4" accounts for 100% of the moment in the Mokoia carbonaceous chondrite, and kamacite with 5-6% nickel accounts for 80-90% of the moment in the chondrites Bjurbole, Mount Brown, Homestead, Barrata, and Cumberland Falls. The remaining 20-10% of the moment is not accounted for.

Impactites contain a wide range of ferromagnetic particle assemblages. Reference to Chao (1968) and El Goresy (1968) and numerous other papers in the volume Shock Metamorphism of Natural Materials (1968) (ed. French and Short) will explain the nature of the opaque mineral fraction in impactites. Lunar samples contain iron particles ranging from $<$ 100 Å to millimeter sizes. Iron is present as spherules and other shapes. There are other phases which may be ferromagnetic but which have not

been studied in any detail. Meteorites, lunar samples, and impactites differ from normal terrestrial samples in the predominance of shape anisotropy due to iron and iron-nickel phases. Discrete mixtures of particles of varying coercivity and/or shape anisotropy cause reduced coercive force and large ratios (R_H) of remanent coercive force (Kneller and Luborsky, 1964; Meikeljohn, 1953) (H_R) to coercive force (H_c) in meteorites, lunar samples, and impactites.

Particle Shape and Saturation Magnetization:

A chondritic meteorite find is usually oxidized to a degree depending on local conditions and time spent on earth. If an Fe sphere is converted to Fe_3O_4 the shape field ($Hs = \frac{4\pi}{3} Is$) changes from $Hs \sim 7000$ Oe to $Hs' \sim 2000$ Oe. This situation is illustrated in Figure 1 where hypothetical magnetization curves for Fe and Fe_3O_4 are shown. The Hs fields, the slopes of the curves, the susceptibility, and the saturation magnetization values (Is) are indicated in the figure. Particle size and shape distributions will introduce curvature in the I vs. H curves for $H < Hs$. It is, however, quite clear that magnetic fields at least 7000 Oersted or greater are needed in studying the extraterrestrial samples. To compare iron bearing samples with terrestrial samples, the effect of the saturation magnetization differences (Δ Is) must be accounted for.

Experimental Results:

Magnetic hysteresis loops and magnetization curves for artificial and natural materials are presented with examples chosen specifically to illustrate the effect of particle shape and composition of the ferromagnetic phases.

Basalt - Sample CH21-001 is a fresh basalt dredged from the Mid Atlantic Ridge. The sample is typical of pillow basalts where a glass crust grades into an aphanitic to crystalline interior. Curve A (Figure 2) corresponds to the glassy crust and curve B to the aphanitic interior. The slopes of the lines AA' and BB' are characteristic of the paramagnetic component in the samples whose slope can be evaluated by considering:

$$\chi_m = A \times 10^{-6} \cdot BX + C(Y + Z) \qquad (1)$$

where A, B, and C are empirical constants and X, Y, and Z are respectively the amounts of Fe^{2+}, Fe^{3+}, and Mn^{2+}. The amount of paramagnetic phase can then be evaluated by

$$C = a + b \cdot 10^6 \chi_m$$

where C is concentration, a and b are constants and χ_m is evaluated as in (1). The same argument holds for all materials. As can be seen in the figure the glassy crust has a significantly larger Hc value than the aphanitic interior which is to be expected since the magnetite grain size distribution varies according to the cooling rate, and the smaller mode is skewed to the glassy crust.

The total amount of ferromagnetic in the aphanitic interior is of course much greater than in the glassy crust, which is reflected in the amount of paramagnetic in the glassy crust. The overall chemical composition of the glassy crust and aphanitic interiors are identical.

Nickel and Iron - Magnetization curves for small rods and spheres illustrate the shape fields (H_S), the influence of the demagnetization factor (N), and the influence of saturation magnetization (I_S). Magnetization curves for a 5mm long Ni wire measured parallel (a) and perpendicular (b) to the rod axis are shown in Figure 3A. The slope of the magnetization curve is 1/N and is the susceptibility in terms of the applied field and is constant until at $H_A=NI_S$ saturation is achieved. When wall coercivity is considered (H_W) then the saturation field is $H_S=NI_S+H_W$.

When two wires (each 5.5 mm long) are crossed the results are quite different as shown in Figure 3B for measurements along the direction (c) parallel to one axis and perpendicular to another, and direction (d) at 45° to the perpendicular wires. Both measurements were made with the applied field in the plane containing the wire axis. Both demagnetizing fields are seen by the magnetometer, e.g., the results shown in Figure 3A. This simulation is important since it has been shown to

be similar to the fusion crust in certain chondrite meteorites (Wasilewski, 1972) where sulfide veins criss cross and/or Fe_3O_4 coexists with metal.

The results for the iron sphere and needle are shown in Figure 4A. The influence of the shape field can be seen by comparing Figure 4A and Figure 3A. If Ni and Fe spheres were mixed together, a resultant curve similar to the crossed Ni wire case (Figure 3B) would be measured since the shape fields for particles with constant N depend on I_S.

Impactite - In the Monturaqui impactite which contains metal grains, as well as magnetic sulfides and oxides, the resultant hysteresis loop is much more complex than the cases in Figure 3 and 4A. In Figure 4B the hysteresis loop for the impactite is shown. Because of the wide variation in I_S and N for the different metal, sulfide, and oxide phases, continuous curvature in the loop is observed for all H_A up to about 6000 Oe. where saturation is achieved.

Particle Agglomeration - The value of N for a sphere is $4\pi/3$ and for a needle of infinite length N is 2π. If the spheres are noninteracting then $N=4\pi/3$ and the shape field is $4\pi I_S/3$. However if the spheres interact then the field H_S is $4\pi I_S(1-f)$ f=packing fraction . If there is any alignment, then the direction of the applied field is important. In Figure 5 are hysteresis

loops for a two sphere configuration where H_A is applied parallel (A) and perpendicular (B) to the axis of the two sphere configuration. The resultant H_S fields are

$$H_S(A) < H_S(S) < H_S(B)$$

where $H_S(S)$ is the shape field $4\pi/3\ I_S$ of a single sphere.

Chondrites - Two L6 chondrites (Wasilewski, 1972) Modoc and Holbrook were studied. Spherical particles and particles of irregular shape are present in both samples. Hysteresis loops for both L6 chondrites are shown in Figure 6A. The R_H value (ratio of H_R to H_c) is 14.6 for Modoc based on H_c=75 Oe. and H_R=1100 Oe. with R_I (ratio of remanent magnetization to saturation magnetization) =0.03. The high R_H value is due to the presence of spherical shaped particles and in general to particles of high NI_S values. A steel sphere (52100) has an R_H value of 16.

Taylor and Heymann (1969) have defined shock classes for chondrite meteorites based on metallographic studies. Hysteresis loops for chondrites which fit three of their shock classes are illustrated in Figure 6B Richardton (Class A), Holbrook (Class B), Calliham (Class D) . These studies are preliminary and though indications are that the shape fields, H_S, change with increasing shock alteration more experimentation is required.

Fusion Crust and Oxidation - Previous research into the magnetic properties of the black fusion crust on chondrite

meteorites (Wasilewski, 1972) indicates complete mineralogical changes and associated thermochemical as well as thermoremanent magnetizations. The example shown in Figure 1, where Fe is oxidized to Fe_3O_4, applies. The R_H and R_I ratios and the field H_S all vary in predictable ways. Any constriction in the chondrite hysteresis loop is also eliminated in the fusion crust.

Shown in Figure 7 are hysteresis loops for the Bowesmont chondrite and the weathered Bowesmont fusion crust. Percentage wise there is a stronger paramagnetic component in the meteorite than in the fusion crust which is to be expected since Fe in the silicate phase is oxidized in the crust, rendering the silicate mass devoid of paramagnetic iron.

Lunar Samples - Nearly all the lunar samples contain superparamagnetic metal. This results in reduced H_c, increase in the R_H value, and constriction in the hysteresis loops. The presence of large multidomain components also reduces H_c and results in an increase in the R_H value. Paramagnetism due to iron in glass and silicate crystals is quite significant in the lunar samples. Shown in Figure 8 are hysteresis loops for lunar samples 10021, 10085, and 10084 (T. Nagata and F. Schwerer private communication). The saturation field (H_S) is $\sim$ 7000 Oe. for the fines (10084), $\sim$ 4000 Oe. for the breccia (10085), and $\sim$ 2000 Oe.

for the breccia powder (10021).

Remanence Ratio and Coercivity - The values of H_c, H_R and the ratios R_H, R_I for some of the samples shown in Figures 2 to 8 are listed in Table I. It has been shown previously that a classification of natural ferromagnetic materials can be made by utilizing the magnetic hysteresis data (Wasilewski, 1972).

Titanomagnetite ($xFe_2 \cdot TiO_4$-1-xFe_3O_4) - For a given particle shape, N is the demagnetization factor, and H_S ($=NI_S$) depends on I_S. For the titanomagnetites the I_S value ranges from $I_S \sim 0$ for $x = 0.8$ to $I_S \sim 480$ emu/cc for $x=0$, at room temperature. For spheres, needles, plates, and ellipsoids the demagnetization factors are well established, but for natural materials the grain shapes are more severe. In particular, in ocean and continental basalts, meteoritic fusion crust, and spherules of cosmic origin dendritic grain shapes are common. Rhodes et al. (1962) have shown that the H_c of dendritic crystals will be smaller than the H_c estimated from dimensions of an equivalent ellipsoid. It has been established that the R_I values increase and R_H values decrease as the grain size decreases for magnetic class I basalts. The influence of composition and size of titanomagnetites on the hysteresis loops is demonstrated in the Figures 9A and 9B. Hysteresis loop squareness depends both on grain size and composition.

Shape Dispersions:

A bimodal mixture of spheres and needles can be distributed in an inert matrix in four ways (Figure 10A). To a first approximation mixture (C) represents a chondrite meteorite. Neglecting the size distribution, all chondrite meteorites consist of a heterogeneous mixture of spherical shaped grains and irregular shaped grains of metal. (In the carbonaceous chondrites this argument does not hold because of the significance of the oxide phases.) Each of the cases (a) to (d) give magnetization curves distinctly different from each other (Figure 10B).

Consider case (a) and (b) which are identical except for a 90° rotation with respect to H_A, the measuring field. The effect due to the spheres remains the same but in case (a) the field sees the hard rod direction and in case (b) the easy direction. The measured curve is a composition curve for a simple two component assemblage (Figure 11).

From a composition curve of this type, assuming a simple two component assemblage, a quantitative assessment of the distribution of components, component anisotropy, and the shape fields can be made. B and B' correspond to the field H_S ($=NI_S$) associated with the needle and A and A' correspond to that for a sphere. The sharpness of the discontinuities at B and A depend

on the behavior of the two components in the region of approach to saturation and the specific shape distributions. Curvature in the regions O to B and B to A correspond to the angular dependence of the needle component with respect to the field and to deviations from sphericity in the case of the spherical component. The slope beyond A is due to two causes: (a) apparent paramagnetism due to finite measuring fields, and (b) a true paramagnetic matrix component. In decomposing an unknown curve of the type shoen in Figure 11 the paramagnetism is evaluated (=χH) as the dashed line, OC, which has the same slope as A"AA"' . The linear extrapolation to the line H=O at A" marks the saturation magnetization of the system as Msp+Mn, where subscripts sp and n correspond to sphere and needle respectively. The extrapolation ABB" allows separation of the total moment into contributions from (a) spherical particles and (b) needles. If the grain shapes are randomly dispersed, then some distribution function must be introduced, and the discretness of the H_S field disappears.

Discussion and Conclusions:

The magnetic hysteresis loops for lunar fines and lunar breccia powder (Figure 8) are quite different from each other. The H_S field for the fines is about 7.5 K.Oe. and about 2 K.Oe. for the breccia powder. This type of analysis does not enable us to evaluate the superparamag-

netism. The following can be said about the samples:

A. Paramagnetism is greater in the breccia sample.

B. Spherical particle shape is a much more significant ferromagnetic component in the fines.

C. Constriction, i.e. reduced coercivity, is found in both samples and is due to mixed components.

A more detailed analysis should provide much more useful information.

Mixtures of discrete size modes of superparamagnetic single domain or multidomain particles, or the presence of the same size modes but different magnetization values will produce significant alterations to the hysteresis loop. The presence of superparamagnetism and large multidomain grains will reduce H_c and result in loop constriction. The shape field or saturation field is defined as $H_S=NI_S$ and the presence of discrete shape modes can be easily detected. Likewise for the same shape but different magnetization values, the difference (ΔI_S) in magnetization values can be detected ($N\Delta I_S$). Any thermomechanical alteration which changes the magnetization values, the shape distribution, the size distribution, or induces structural transformations can be effectively studied by evaluating magnetization curves and hysteresis loops.

ACKNOWLEDGEMENTS

This work was done during the summer of 1971 while the author held an ASEE-NASA Summer Faculty Fellowship. Thanks are extended to Dr. Emad and Dr. Morakis for their assistance during the program tenure.

Thanks are also extended to Dr. French and Dr. Walter of the Planetology Branch for their assistance and for providing a stimulating environment to conduct research.

TABLE I

Sample	H_C	H_R	R_H	R_I	Note
SAE 52100	50	800	16		steel sphere
Monturaqui	90	225	2.5	.07	impactite
Modoc	75	1100	14.6	.03	L6 chondrite
Calliham	165	270	1.6	.27	metal shock class D
10021	24	410	17.1		breccia powder, lunar
10084	36	460	12.8	.07	fines, lunar
10085	125	670	5.4	.15	breccia, lunar

FIGURE CAPTIONS

Figure 1 - Simplified magnetization curve for an iron sphere and magnetite sphere. The shape field ($H_S=4/3\pi \cdot I_S$) and magnetization values are indicated.

Figure 2 - Hysteresis loops for specimens from a sample of quenched ocean basalt. As one proceeds inward from the glassy crust to the aphanitic and crystalline interior the paramagnetism, coercivity, and hysteresis change in systemmatic fashion.

Figure 3 - Magnetization curves for nickel needles and crossed nickel needles.
A. Magnetization curves parallel and perpendicular to the axis of a 5 mm needle.
B. Magnetization curves (a) along the axis of one needle and perpendicular to the other for the crossed needle set and (b) at an angle 45° to mutually perpendicular needles.

Figure 4 - Hysteresis loops for iron needle, steel sphere, and Monturaqui impactite.
A. Hysteresis loops for steel sphere and for the case parallel to the needle axis.
B. Hysteresis loop for Monturaqui impactite.

Figure 5 - Hysteresis loops for a two sphere configuration measured (a) parallel and (b) perpendicular to elongation. This demonstrates the effect of interaction on the shape field. Similar interacting configurations are found in lunar samples and chondrite meteorites.

Figure 6 - Hysteresis loops for chondrite meteorites.
A. Hysteresis loops for L6 chondrites , Modoc and Holbrook.
B. Hysteresis loops for meteorites with progressive shock metamorphism in the metal phases. A,B,D on curves refer to Taylor and Heymann (1969) metal shock classes.

Figure 7 - Hysteresis loops for the fusion crust and meteorite body - Bowesmont chondrite. The ferromagnetic component for the crust is $(FeNi)_3O_4$ and for the meteorite, FeNi alloy. This analysis reveals that oxidation of FeNi to $(FeNi)_3O_4$ shifts the shape field H_S, increases R_I, and decreases R_H.

Figure 8 - Magnetic hysteresis loops for lunar samples (T. Nagata and F. Schwerer), showing the variation in H_S, R_H, and the significance of the paramagnetic component compared to the ferromagnetic component (see Figure 11).

Figure 9 - Hysteresis ratios for basalts and synthetic titanomagnetite.
A. R_I vs. R_H for basaltic rocks of constant composition but variable size modes.
B. R_I vs. R_H for synthetic titanomagnetite of variable composition, but constant grain size.

Figure 10- Schematic distributions of spheres and needles and the corresponding magnetization curves, b based on the shape field for discrete components and experimental observations.
A. Four possible needls-sphere configurations.
B. Magnetization curves for each of the above configurations.

Figure 11- Schematic analysis of two components A and B with different shape factors. The component curves are normalized for simplicity.

FIGURE 1

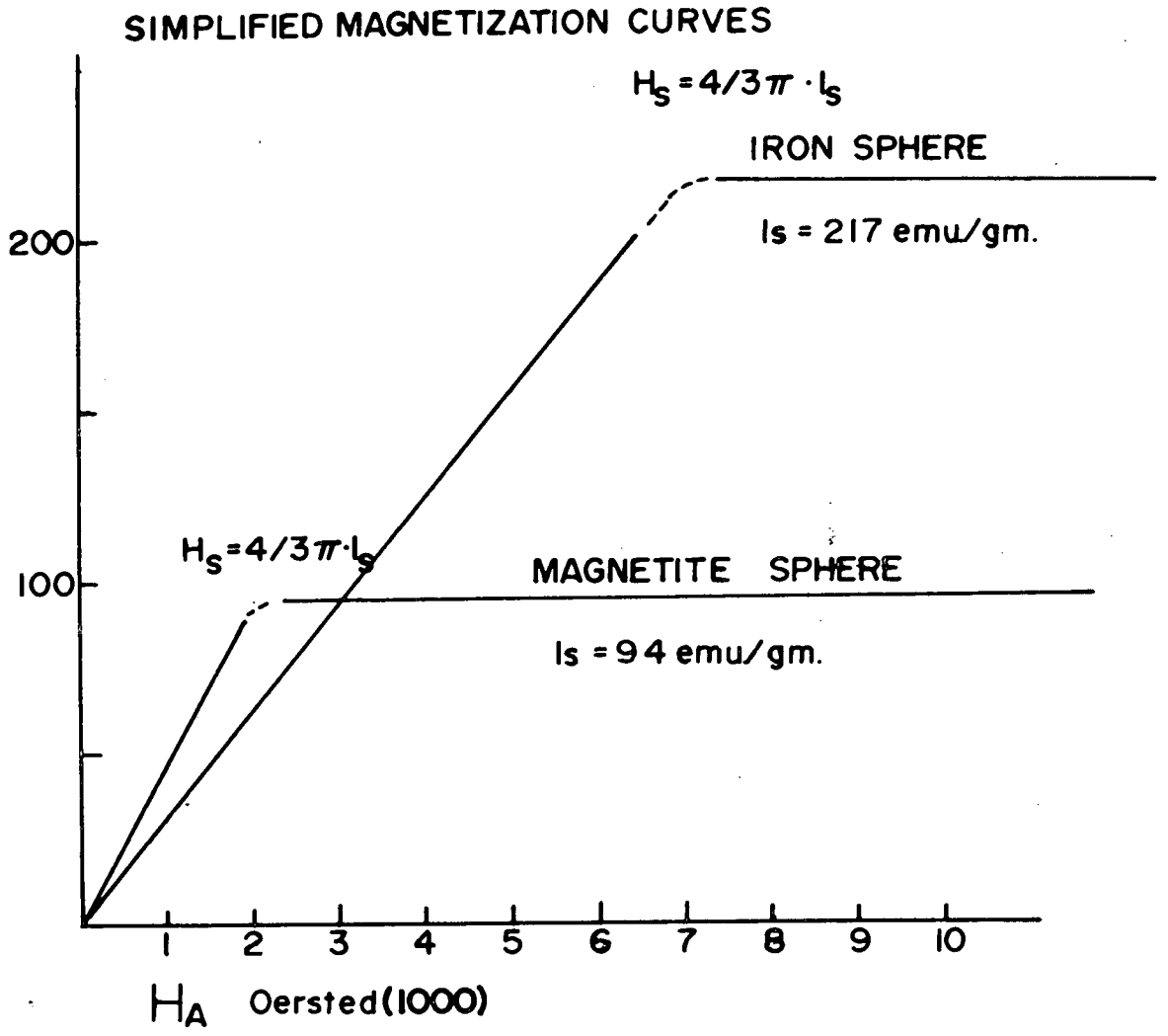
SIMPLIFIED MAGNETIZATION CURVES
$H_S = 4/3\pi \cdot I_S$
IRON SPHERE
Is = 217 emu/gm.
200
100
$H_S = 4/3\pi \cdot I_S$
MAGNETITE SPHERE
Is = 94 emu/gm.
1
2
3
4
5
6
7
8
9
10
H_A Oersted(1000)

FIGURE 2

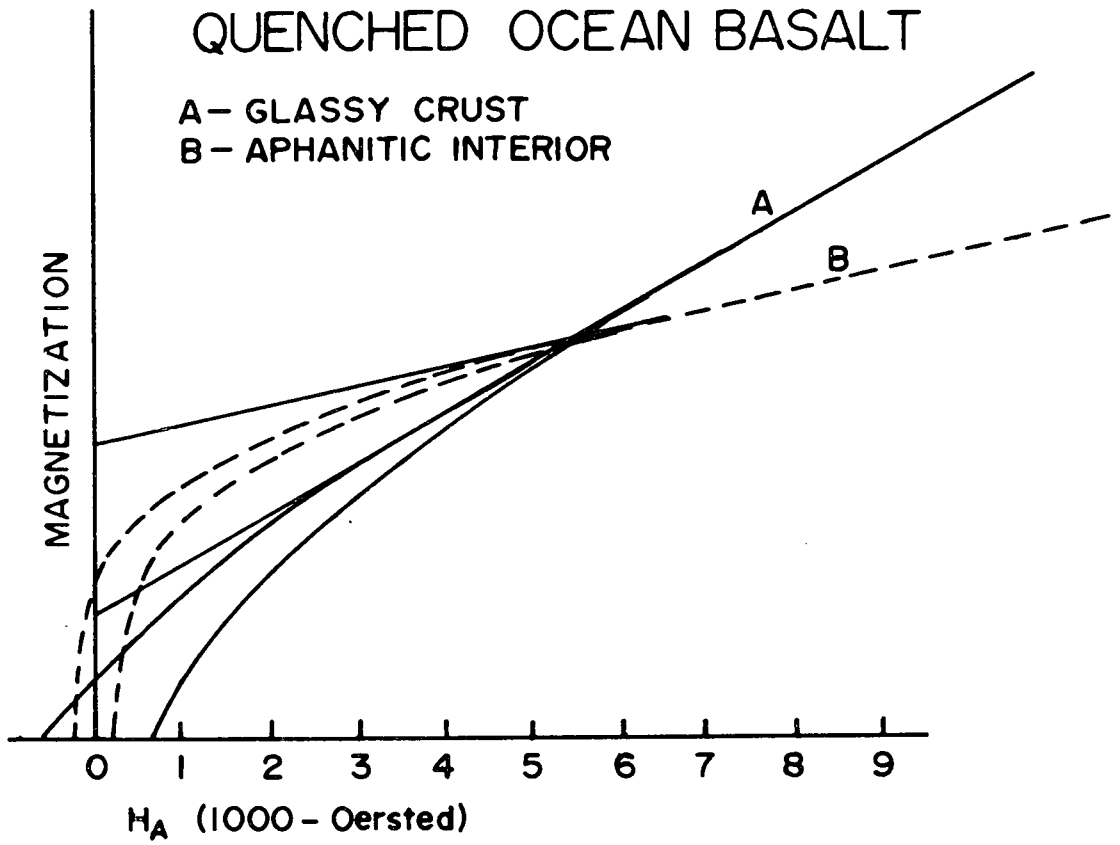
QUENCHED OCEAN BASALT
A – GLASSY CRUST
B – APHANITIC INTERIOR
A
B
MAGNETIZATION
0
1
2
3
4
5
6
7
8
9
H_A (1000 – Oersted)

FIGURE 3

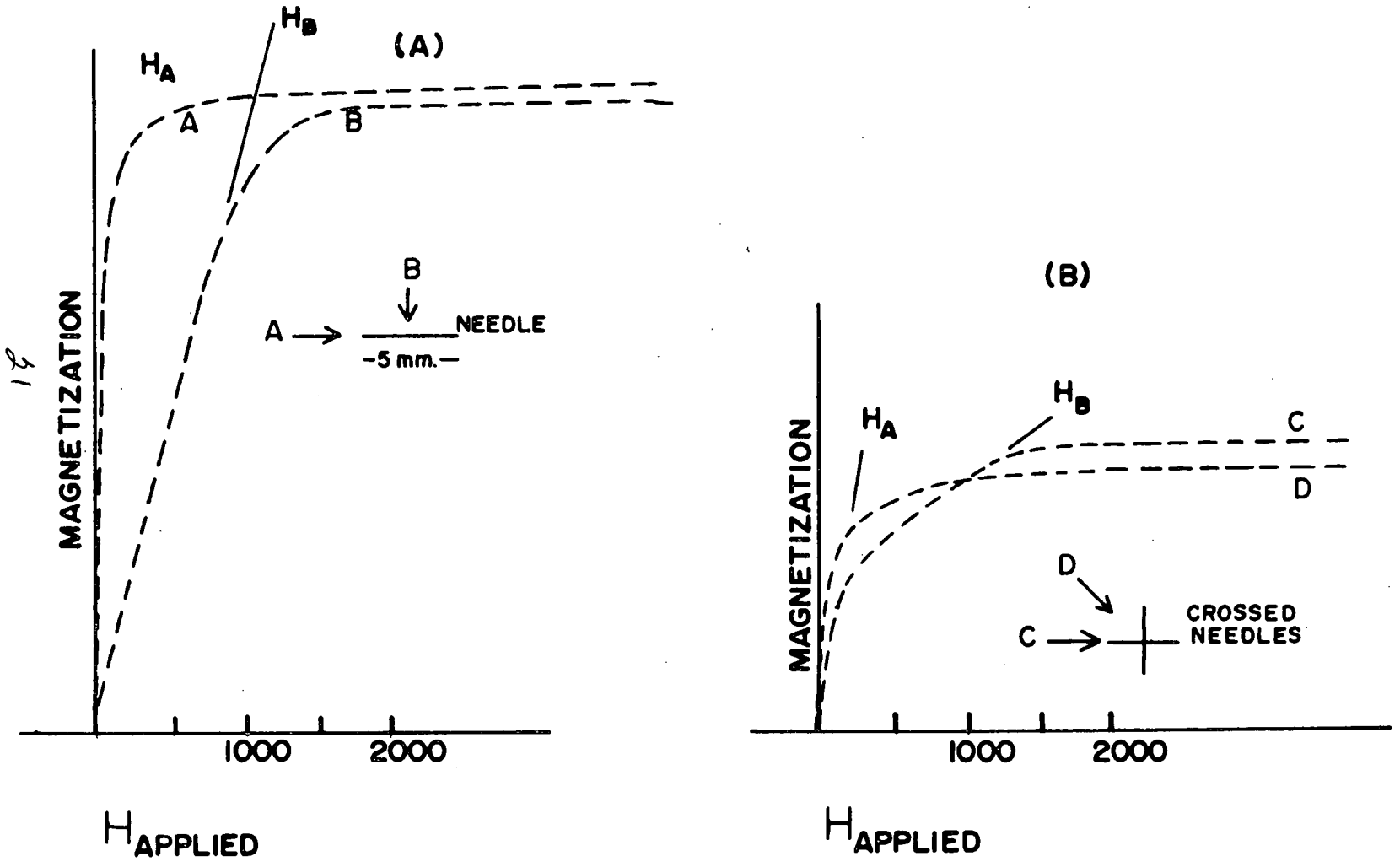
(A)
H_B
H_A
A
B
B
A
NEEDLE
-5 mm.-
MAGNETIZATION
1000
2000
$H_{APPLIED}$
(B)
H_B
H_A
C
D
D
C
CROSSED
NEEDLES
MAGNETIZATION
1000
2000
$H_{APPLIED}$

FIGURE 4

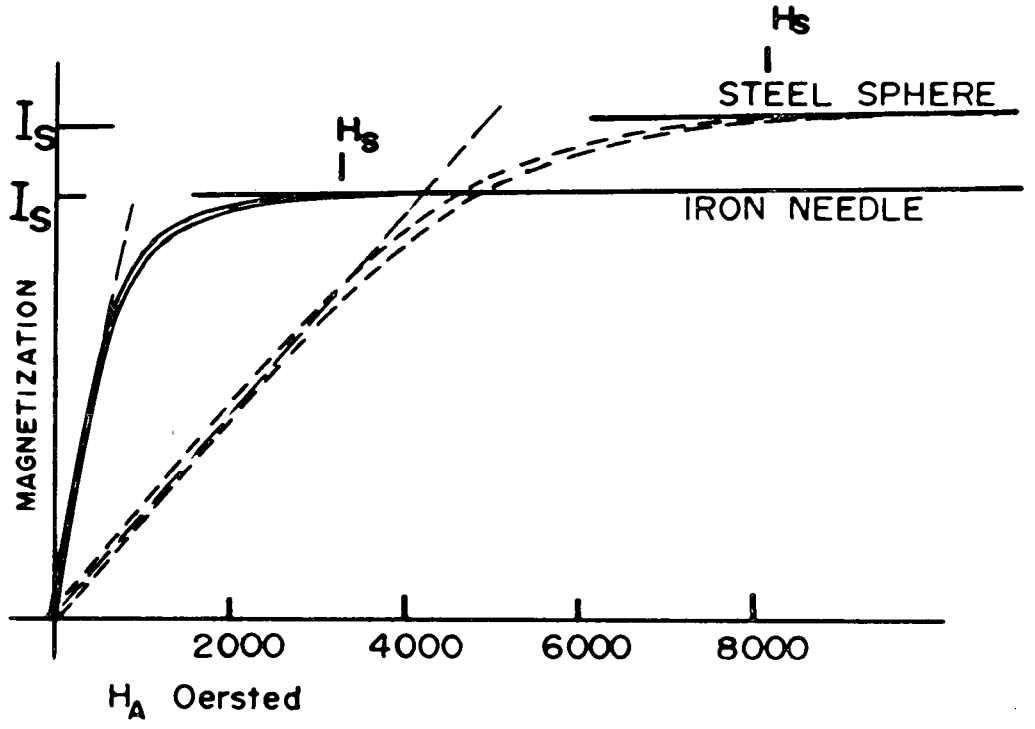
H_s
STEEL SPHERE
I_s
H_s
I_s
IRON NEEDLE
MAGNETIZATION
2000
4000
6000
8000
H_A Oersted

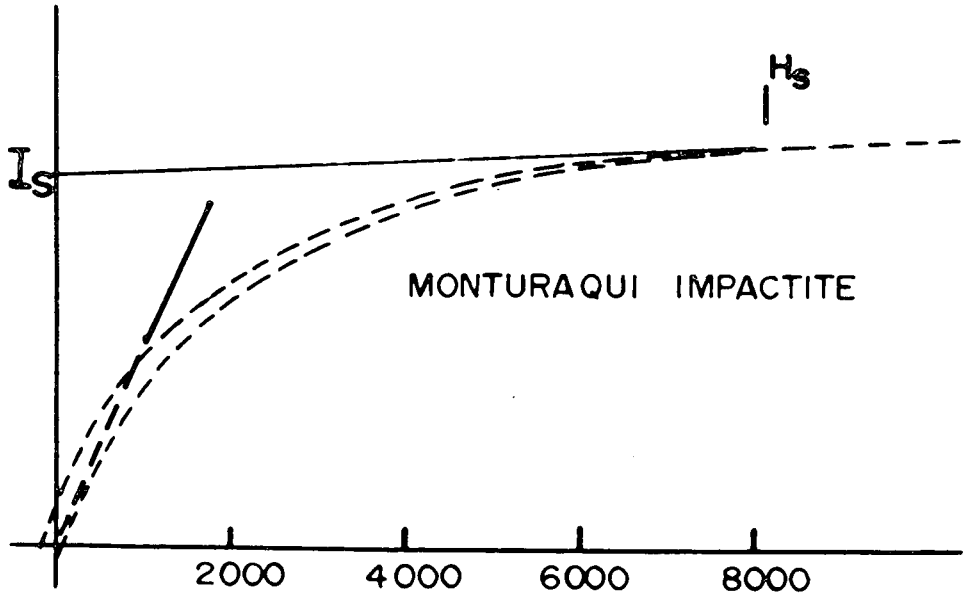
H_s
I_s
MONTURAQUI IMPACTITE
2000
4000
6000
8000

FIGURE 5

TWO SPHERE CONFIGURATION
ILLUSTRATION OF THE EFFECT OF INTERACTION ON
THE EFFECTIVE SHAPE FIELDS

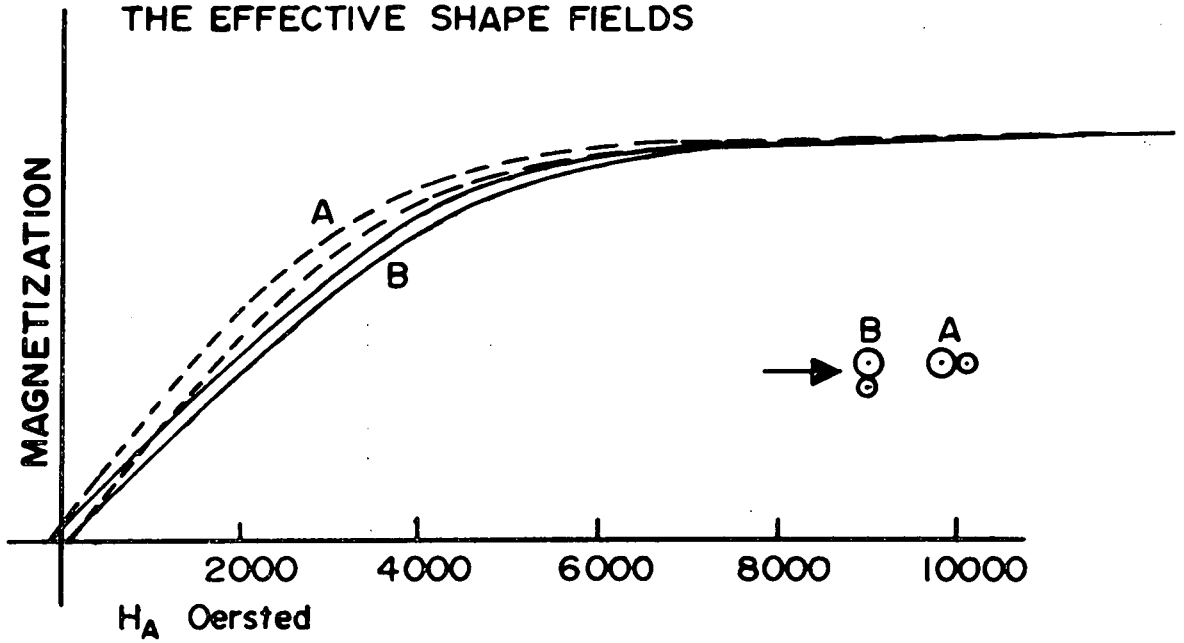

FIGURE 6

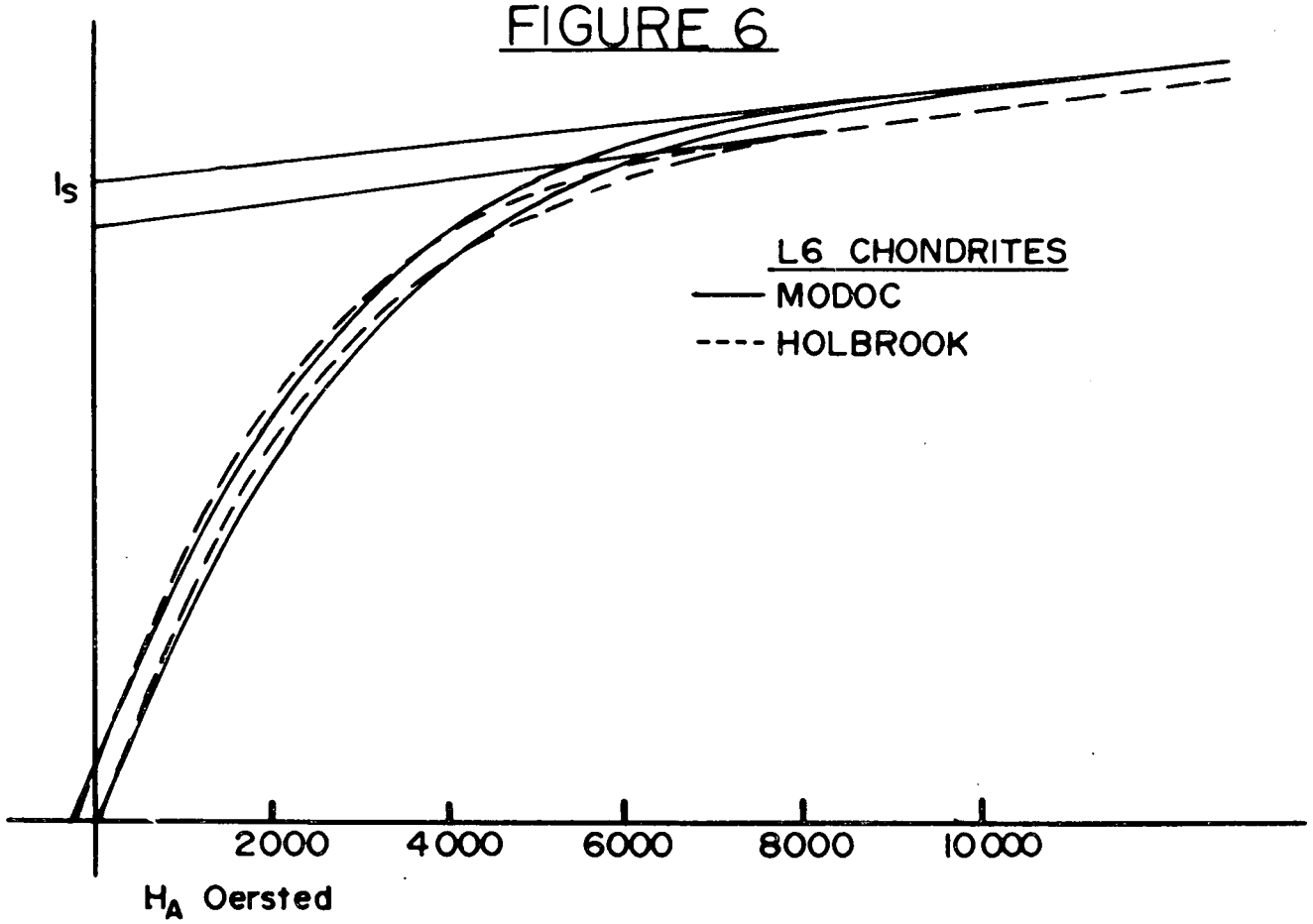
I_S
L6 CHONDRITES
MODOC
HOLBROOK
2000
4000
6000
8000
10000
H_A Oersted

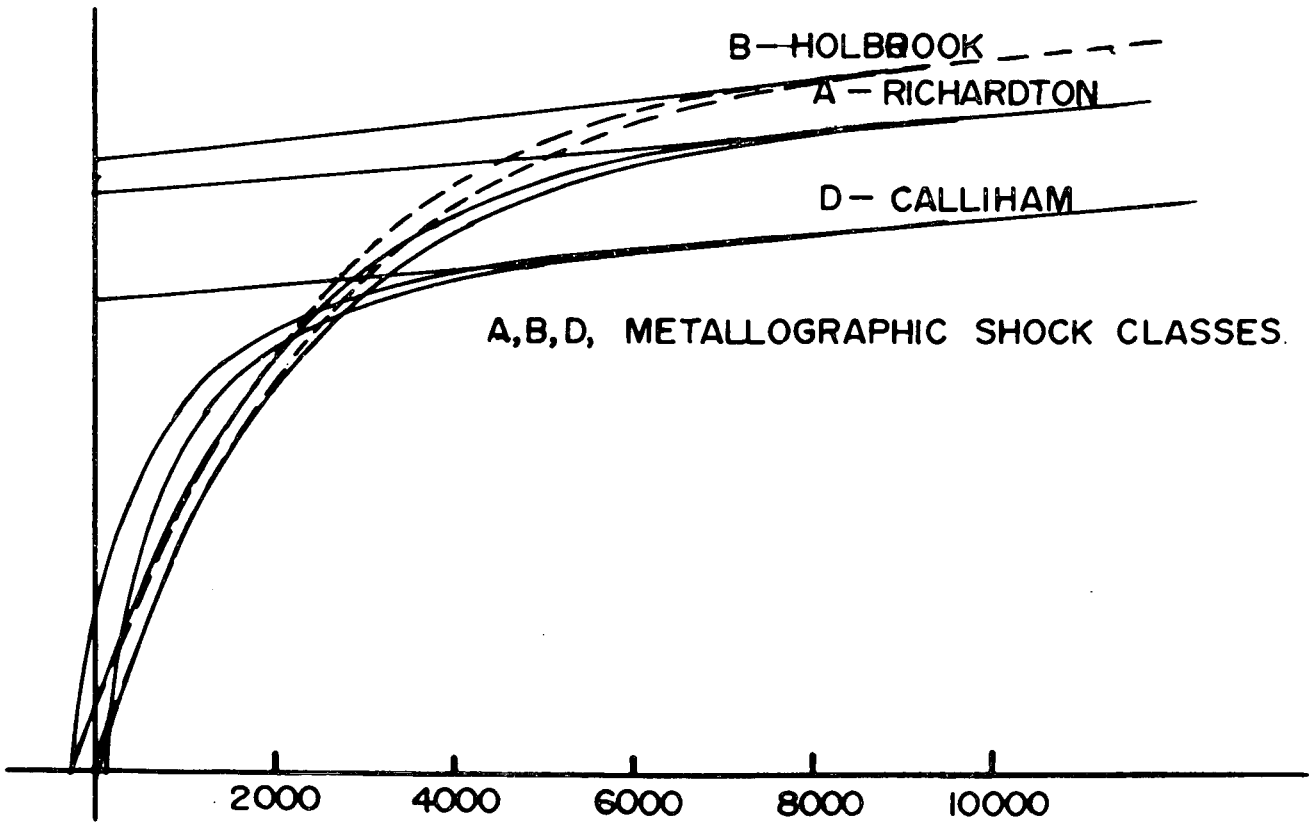
B—HOLBROOK
A—RICHARDTON
D—CALLIHAM
A,B,D, METALLOGRAPHIC SHOCK CLASSES
2000
4000
6000
8000
10000

FIGURE 7

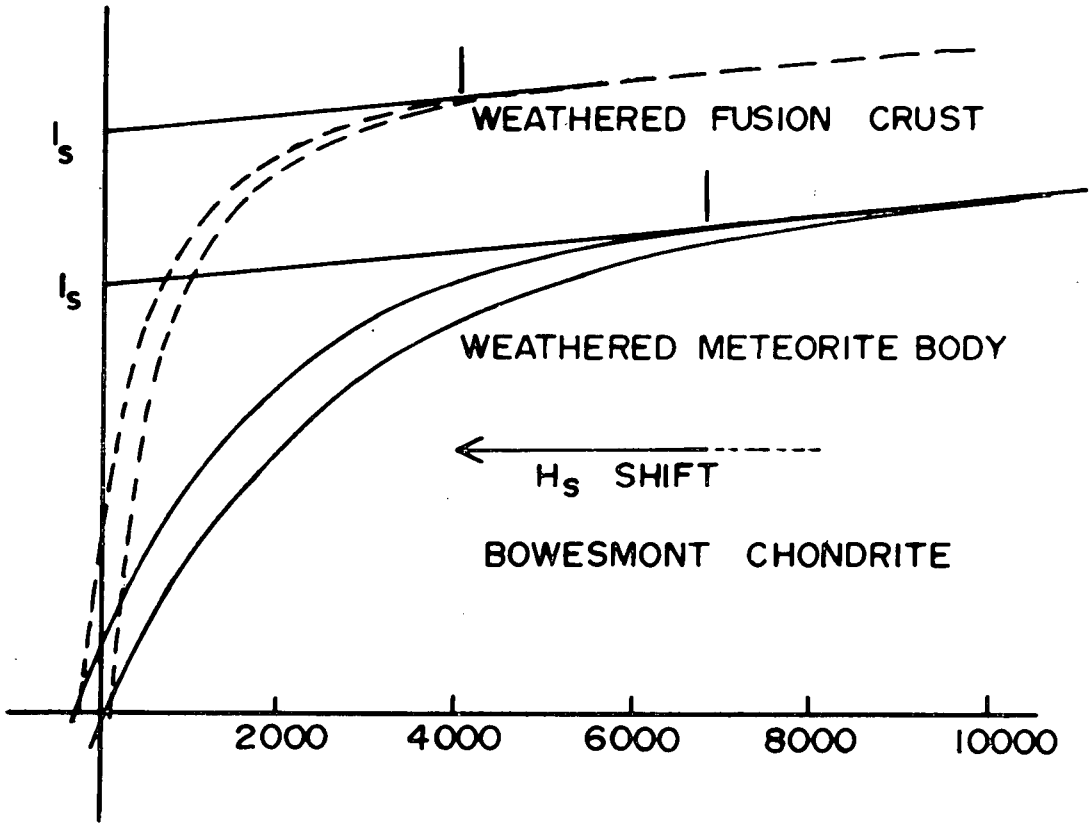

FUSION CRUST — FERROMAGNETIC COMPONENT IS MAINLY $(FeNi)_3O_4$

METEORITE BODY — MAINLY FeNi, OXIDIZED FeNi, $Fe_{1-S}S$

FIGURE 8

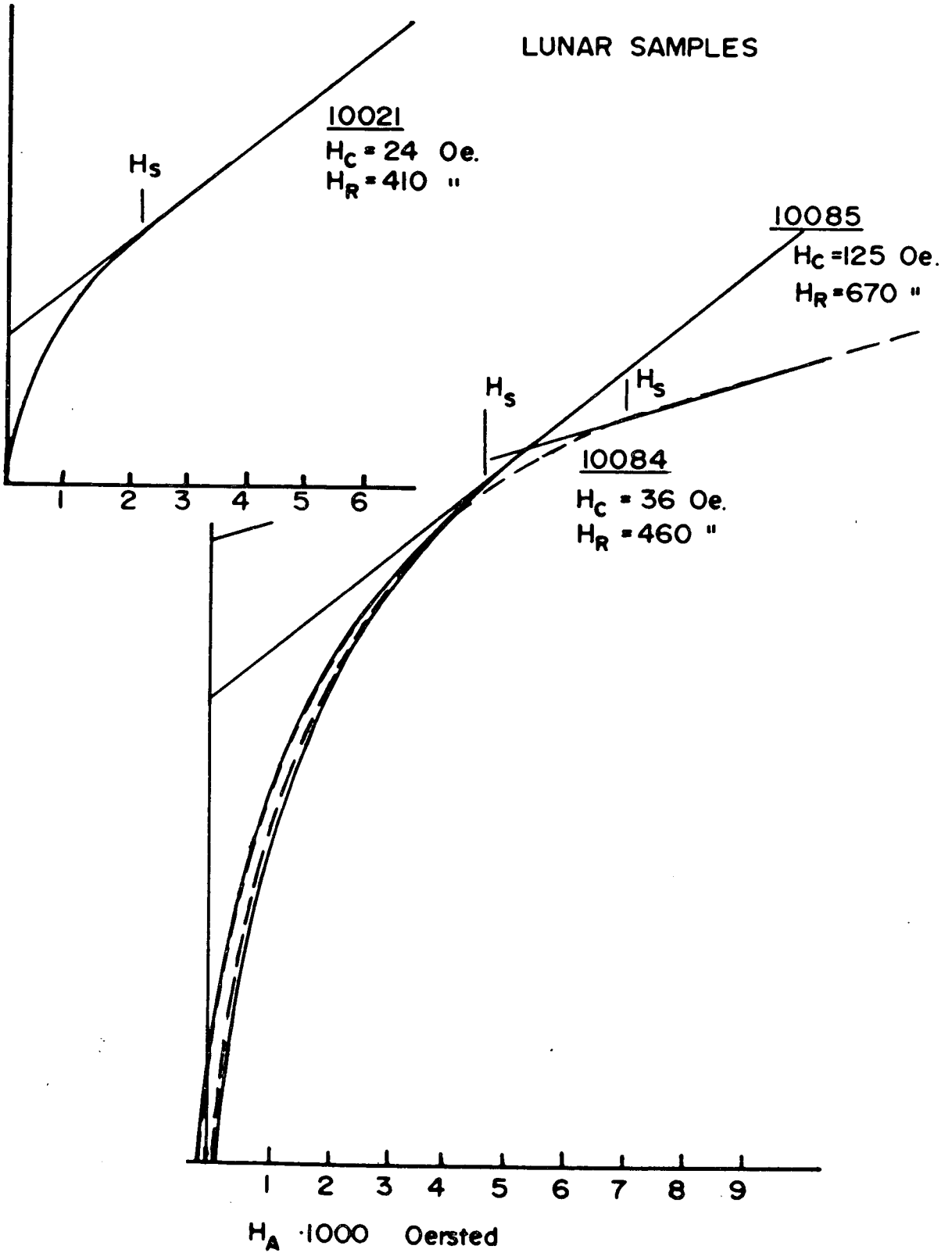
LUNAR SAMPLES
10021
H_C = 24 Oe.
H_R = 410 "
H_S
10085
H_C = 125 Oe.
H_R = 670 "
H_S
H_S
10084
H_C = 36 Oe.
H_R = 460 "
1 2 3 4 5 6
1 2 3 4 5 6 7 8 9
H_A ·1000 Oersted

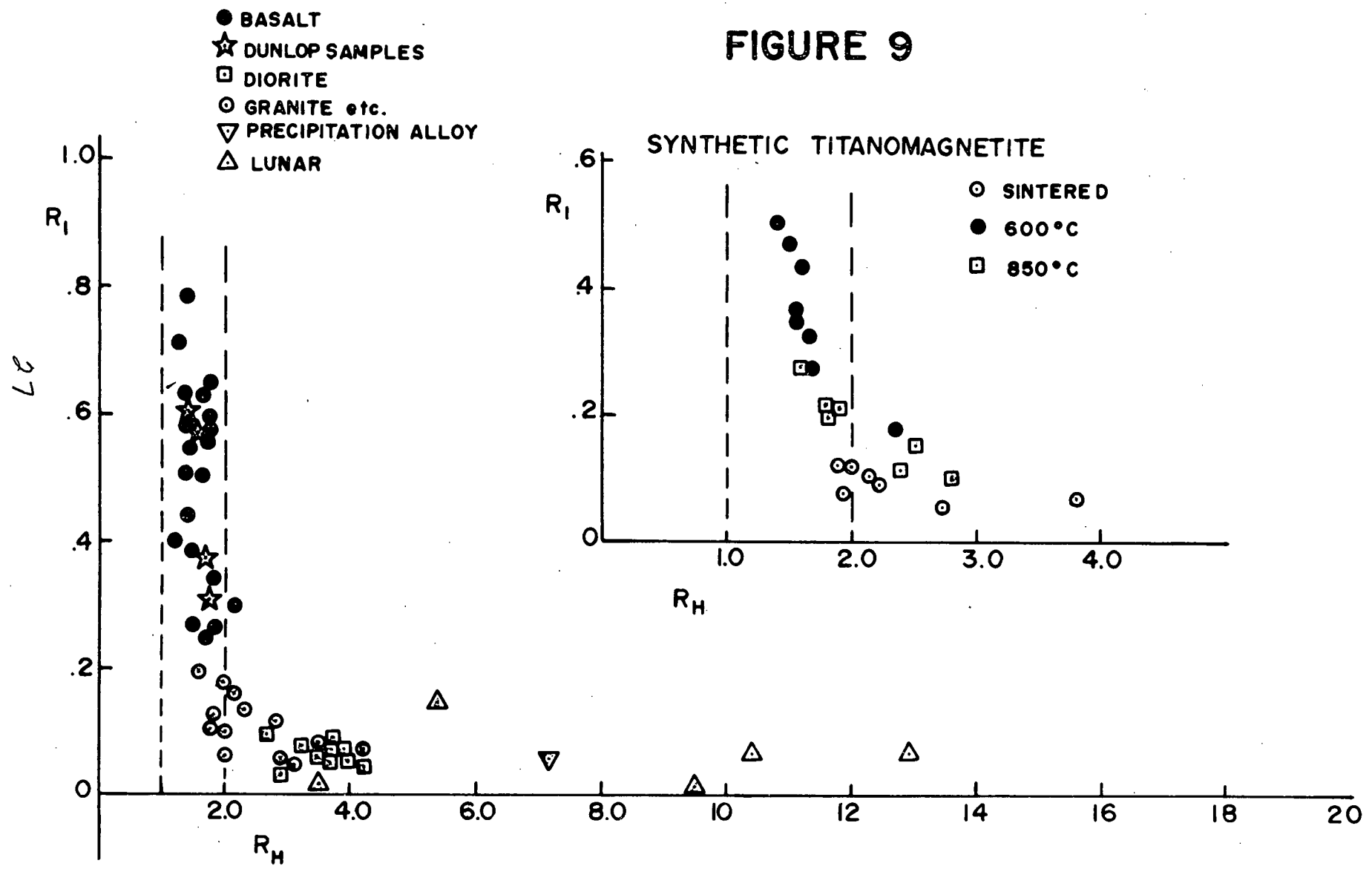
BASALT
DUNLOP SAMPLES
DIORITE
GRANITE etc.
PRECIPITATION ALLOY
LUNAR
SYNTHETIC TITANOMAGNETITE
SINTERED
600°C
850°C
R_I
R_H
1.0
.8
.6
.4
.2
0
2.0
4.0
6.0
8.0
10
12
14
16
18
20
3.0

FIGURE 9

HYPOTHETICAL MAGNETIZATION CURVES

SPHERE COMPONENT IN ALL DISTRIBUTIONS

H_S (needle⊥) > H_S (sphere) > H_S (needle ∥)

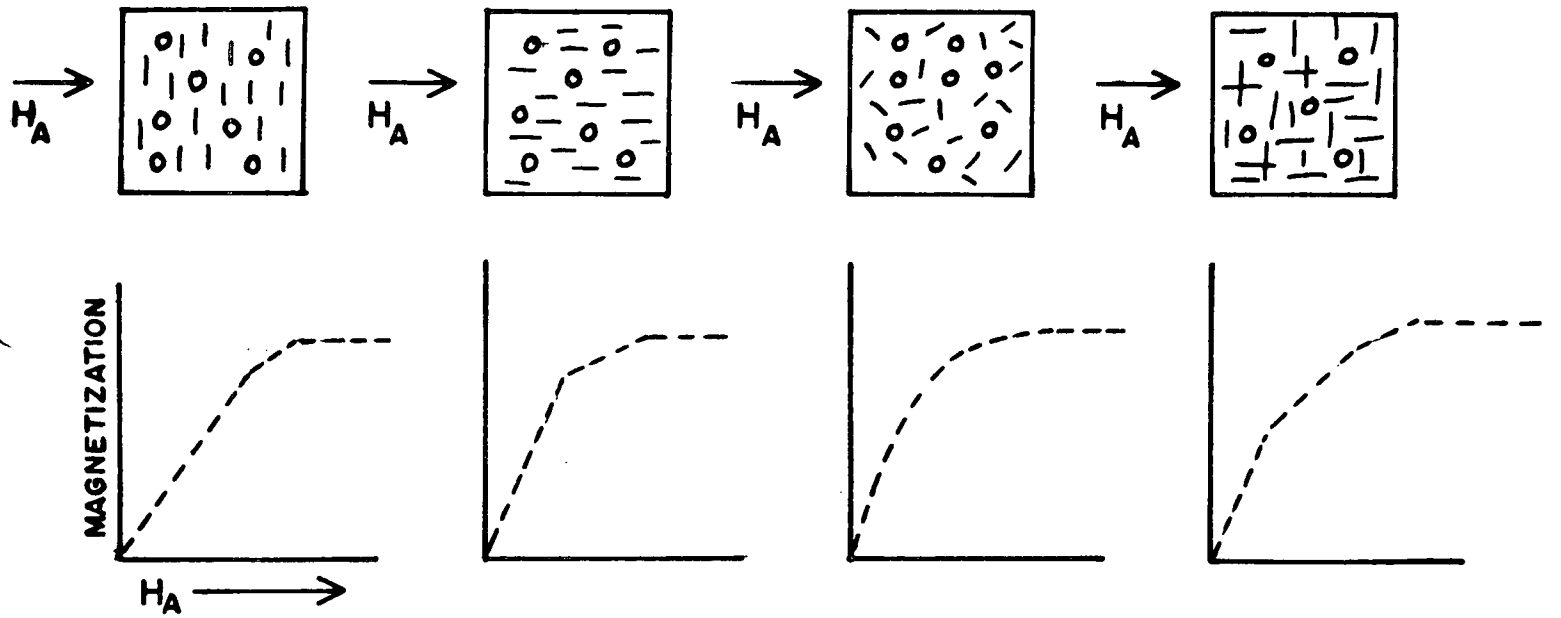

IF GRAIN SHAPE IS DISCRETE - DISCONTINUITIES ALLOW FOR EVALUATION OF H_S - AND THE APPARENT HARDNESS.

FIGURE 10

FIGURE II

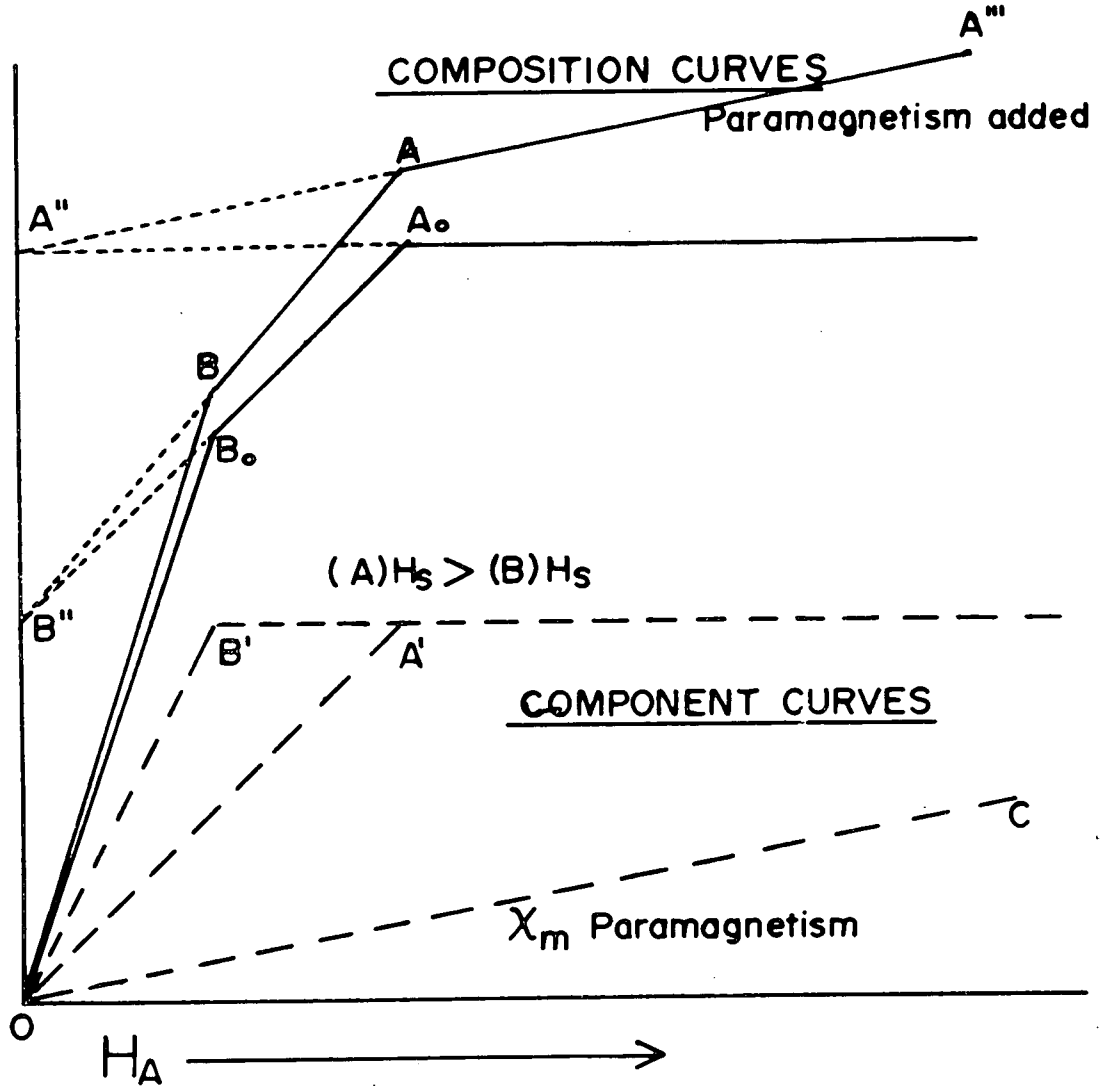

TWO COMPONENTS A, AND B OF EQUAL MAGNETIZATION BUT DIFFERENT SHAPE FACTORS

REFERENCES

Chao, E. C. T., 1968, Pressure and temperature histories of impact metamorphosed rocks-based on petrographic observations: in Shock Metamorphism of Natural Materials, edited by B. M. French and N. M. Short, Mono Book Corp., Baltimore.

El Goresy, A., 1968, The opaque minerals in impactites glasses: in Shock Metamorphism of Natural Materials, edited by B. M. French and N. M. Short, Mono Book Corp., Baltimore.

French, B. M., and N. M. Short, 1968, Shock Metamorphism of Natural Materials, Mono Book Corp., Baltimore.

Kneller, E. F., and F. E. Luborsky, 1963, Particle size dependence of coercivity and remanence of single domain particles: Jour. Appl. Phys., V34, p656.

Meikeljohn, W. H., 1953, Experimental study of the coercive force of fine particles: Rev. Mod. Phys., V25, p302.

Rhodes, P.,G. Rowlands, and D. R. Birchall, 1962, Magnetization energies and distributions in ferromagnetics: Jour. Phys. Soc. Japan, V17 (B1), p543.

Stacey, F. D., J. F. Lovering, and L. G. Parry, 1961, Thermomagnetic properties, natural magnetic moments, and magnetic anisotropy of some chondritic meteorites: Jour. Geophys. Res., V66, p1523.

Taylor, G. J., and D. Heymann, 1969, Shock reheating and gas retention ages of chondrites: Earth & Planet. Sci. Lett., V7, p151.

Wasilewski, P., 1972, Magnetic hysteresis in natural materials: to be published in Earth & Planet. Sci. Lett.

Wasilewski, P., 1972; Magnetic properties of chondrite meteorite fusion crust: NASA-Goddard Space Flight Center, X Document, X 644-72-163.

Wasilewski, P., 1972, Magnetic hysteresis in chondrite meteorites: NASA-Goddard Space Flight Center, X Document, X 644-72-167.